Synthesis Routes for Bioactive Sol−Gel Glasses: Alkoxides versus Nitrates

A. Rámila, F. Balas, and M. Vallet-Regí*

Departamento de Química Inorgánica y Bioinorgánica, Facultad de Farmacia, UCM E-28040, Madrid, Spain

Received March 14, 2001. Revised Manuscript Received October 16, 2001

The synthesis of a new bioactive glass with a composition in mol % of 76% SiO_2, 23% CaO, and 1% P_2O_5 was achieved by the sol−gel method with the employment of two different pathways: via inorganic salts (**76S**) and via metal alkoxides (**76SA**). The in vitro bioactivity of both glasses was assessed by soaking them in simulated body fluid for different time periods, and the changes in the texture were analyzed. Comparison of glasses synthesized by the two pathways was also carried out. Although both show good bioactivity, glass synthesized via metal alkoxides leads to the formation of a more homogeneous apatite layer on its surface. In addition, this newly formed layer is thicker and more compact for **76SA**, and the homogeneous nucleation of the apatite on the surface leads to a better bond between glass and the mentioned newly formed layer.

Introduction

In the past 3 decades, glasses have been widely used in technology due to their many applications as monoliths, fibers, or coatings. Hence, a relevant application of glasses is being done in the field of biomaterials.[1,2]

Glasses with the ability to bond with living tissues without forming an encapsulating layer of dead cells are usually called bioactive.[3,4] When bioactive glasses make contact with biological fluids, an amorphous calcium phosphate layer is crystallized and an apatite-like structure is formed.[5,6] The apatite crystals, reinforced with collagen fibers, form the bonding layer between bioactive glasses and living tissues.

This formation of an apatite layer is also detected when bioactive glasses are soaked in solutions mimicking the human plasma. Therefore, in vitro assays are extensively used to design new glasses to be used as implants.

There are well-known methods for producing glasses: melting,[7] sintering,[8] and sol−gel.[9] The former consists of melting a mixture of inorganic compounds (oxides, carbonates, phosphates, etc.) and quenching the melt, while the sintering implies the consolidation of amorphous powder to form pure glass. On the other hand, the sol−gel method consists of obtaining the sol by condensation of the precursors and gelation of this sol. The sol−gel method presents some advantages with respect to melting. In first place, glasses are obtained with a higher degree of purity, with more varied compositions and with better homogeneity.

Besides, the sol−gel procedure can employ inorganic salts or alkoxides as reagents. Precursors of SiO_2 and P_2O_5 are usually alkoxides due to their availability, whereas inorganic salts are generally used to generate the calcium component. In fact, there are only occasional references about sol−gel preparation using calcium alkoxides.[10] However, the use of calcium nitrate (which is the standard reagent employed) presents some disadvantages such as the need of removal of nitrates. This process of elimination can alter glass structure and textural properties that could further affect its bioactive behavior.[11−13]

This paper presents the results of an investigation on new potential bioactive glasses that are obtained by the sol−gel method employing two different procedures: inorganic and organometallic routes. A comparative analysis of the as-obtained glasses was carried out to determine the possible benefits of employing metal alkoxides. In addition, the in vitro bioactivity of both glasses was achieved and differences between both processes were pointed out.

Also, the calcium alkoxide employed in the organometallic route was synthesized immediately before the glass synthesis, to ensure its purity and freshness.[14]

Experimental Section

Glass Synthesis Procedure. Glass composed of (mol %) of 76% SiO_2, 23% CaO, and 1% P_2O_5 was prepared by the sol−

* To whom correspondence should be addressed. Tel: 34913941861. Fax: 34913941786. E-mail: vallet@farm.ucm.es.

(1) Hench, L. L. *J. Am. Ceram. Soc.* **1998**, *81*, 1705.
(2) Ducheyne, P. *MRS. Bull.* **1998**, *23*, 43.
(3) Hench, L. L.; Kokubo, T. *Handbook of Biomaterials Properties*; Black, J., Hastings, G., Eds.; Chapman & Hall: London, 1998; p 355.
(4) Bajpai, P. K.; Billote, W. G. *The Biomedical Engineering Handbook*; Bronzino, J. D., Ed.; CRC Press: University of Iowa, 1995; p 552.
(5) Hench, L. L. *J. Am. Ceram. Soc.* **1991**, *74*, 1487.
(6) Kokubo, T. *An. Quim. Int. Ed.* **1997**, *93*, S49.
(7) Zarzycki J. *Glasses and the Vitreous State*; Cambridge University Press: Cambridge, 1991.
(8) Rabinovich, E. M. *J. Mater. Sci.* **1985**, *20*, 4259.
(9) Brinker C. J.; Scherer G. W. *Sol−gel Science. The Physics and Chemistry of Sol−Gel Process*; Academic Press: San Diego, 1990.
(10) Pereira, M. M.; Clark, A. E.; Hench, L. L. *J. Mater. Synth. Process.* **1994**, *2*, 189.
(11) Vallet-Regí, M.; Romero, A. M.; Ragel, V.; LeGeros, R. Z. *J. Biomed. Mater. Res.* **1999**, *44*, 416.
(12) Vallet-Regí, M.; Rámila, A. *Chem. Mater.* **2000**, *12*, 961.
(13) Vallet-Regí, M.; Balas, F.; Pérez-Pariente, J. *Chem. Mater.* **2000**, *12*, 750.
(14) Bradley, D. C. *Chem. Rev.* **1989**, *89*, 1317.

10.1021/cm0110876 CCC: $22.00
Published on Web 02/01/2002

gel method employing two different pathways: via inorganic route (**76S**) and via organometallic route (**76SA**).

76S glass was synthesized by employing tetraethyl orthosilicate (TEOS), triethyl phosphate (TEP), and calcium nitrate as reagents. The glass was prepared by hydrolysis and polycondensation of TEOS (16.5 mL), TEP (0.34 mL), and $Ca(NO_3)_2 \cdot 4H_2O$ (7.79 g), in stoichiometric amounts, to obtain the desired composition. HNO_3 (2 N) was used to catalyze the hydrolysis of TEOS and TEP, using a molecular ratio of $(HNO_3 + H_2O)/(TEOS + TEP) = 8$. After the addition of each reactant, the solution was stirred for 1 h, and the resulting sol was introduced into a hermetically sealed cylindrical Teflon container for 3 days to allow the gel formation. The gel was then aged at 70 °C for 3 days and dried at 150 °C for 48 h. This latter step was carried out after making a 1 mm diameter hole in the lid, to allow leakage of gases. The dried gel was ground and sieved, taking the grains ranging in size from 32 to 63 μm. Fractions of 0.5 g of powder were compacted at 50 MPa of uniaxial pressure and 150 MPa of isostatic pressure to obtain disks (13 mm in diameter and 2 mm in height). To determine the stabilization temperature at which the components form a homogeneous glass and no other mass loss is detected, thermogravimetric and differential thermal analyses (TG/DTA) of the dried gel were carried out, and then gel disks were sintered at 700 °C for 3 h. The transformation temperatures obtained were 575 and 350 °C for **76S** and **76SA**, respectively.

The synthesis of **76SA** was carried out by utilizing tetraethyl orthosilicate (TEOS), triethyl phosphate (TEP), and 2-methoxyethane calcium alkoxide. Since calcium alkoxides are very easily hydrolyzed when in contact with atmospheric humidity, the mixing of the reactants has to be done under nitrogen atmosphere. Hence, mentioned amounts of TEOS and TEP were stirred together for 1 h and 31.39 mL of a solution of 2-methoxyethane calcium alkoxide in 2-methoxyethanol (20% w/v) was then added. After 1 h of being stirred, the sol was allowed to hydrolyze by introducing it inside a hermetic container together with 100 mL of water at 25 °C for 7 days. The gel obtained was aged at 70 °C for 3 days, and the recovered dark yellow monoliths were dried at 150 °C for 3 days. The disks and the stabilization temperature were obtained as explained above. In this case, a temperature of 375 °C was sufficient to sinter the disks considering that no thermal changes were detected upon thermal treatment at higher temperature.

The 2-methoxyethane calcium alkoxide employed in the synthesis of **76SA** was obtained by the reaction of Ca and 2-methoxyethanol, in stoichiometric amounts, refluxed for 10 h in hexane as solvent. Afterward, hexane was removed at reduced pressure and the obtained alkoxide was immediately employed in **76SA** synthesis to avoid its hydrolysis. 2-methoxyethane calcium alkoxide was characterized by FTIR (KBr): $\nu = 470$ cm^{-1} (Ca−O), no OH band was detected.

Figure 1 shows a scheme of both methods.

In Vitro Assay. The assessment of in vitro bioactivity was carried out in simulated body fluid (SBF), which has the same composition and ionic concentration as that of human plasma.[15] The SBF was prepared by dissolving the following reagent chemicals in bidistilled water: NaCl (7.996 g), $NaHCO_3$ (0.350 g), KCl (0.224 g), $K_2HPO_4 \cdot 3H_2O$ (0.228 g), $MgCl_2 \cdot 6H_2O$ (0.305 g), 1 N HCl (40 mL), $CaCl_2$ (0.278 g), Na_2SO_4 (0.071 g), and $NH_2C(CH_2OH)_3$ (6.057 g). The solution was kept at 37 °C, and pH was adjusted to 7.3−7.4. The in vitro assays were carried out by soaking the disks, mounted vertically in a special platinum scaffold, in 45 mL of SBF in polyethylene containers maintained at 37 °C.

Evolution of the disk-shaped glasses immersed in SBF was followed by analysis of the SBF solution (Ca^{2+}, P, and pH) on a Ilyte $Na^+K^+Ca^{2+}$ pH system, and the newly formed layer was characterized by FTIR, in a Nicolet Magna-IP spectrometer 550, scanning electron microscopy and energy dispersive spectroscopy (SEM-EDS), in a JEOL 6400 microscope at 20 kV, XRD, in a Philips X'Pert MDP diffractometer, N_2 adsorption, on a Micromeritics ASAP 2110 instrument, and Hg porosimetry, on a Micromeritics Autopore III 9420 instrument. The XRD, SEM, and EDS studies were carried out directly on the surface of the glass without any treatment. Thermogravimetric analysis were carried out on a Seiko thermobalance TG/DTA 320. The reagents employed were provided by Aldrich.

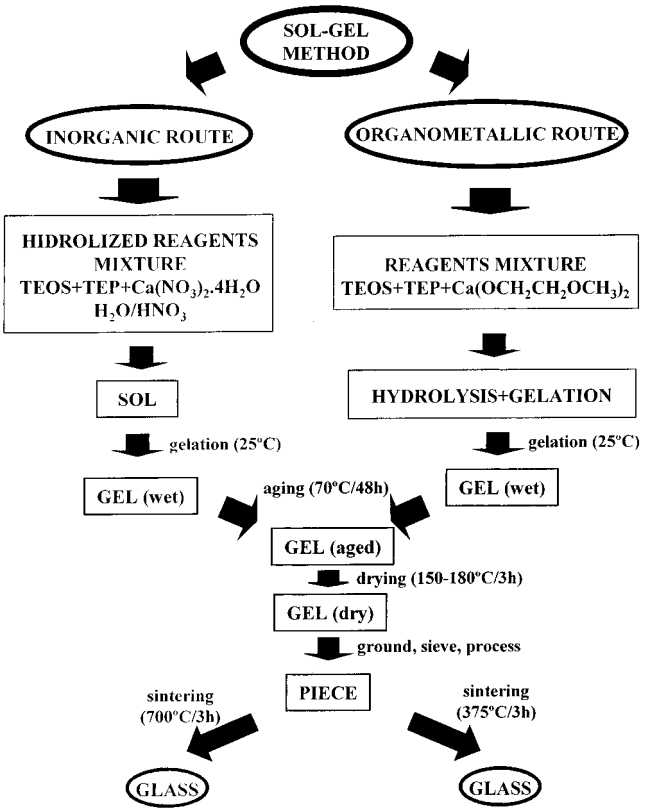

Figure 1. Sol−gel method via inorganic salts and via metal alkoxides.

Results and Discussion

Formation of the Apatite-like Layer. FTIR spectra of **76S** and **76SA** before and after soaking in SBF are shown in Figure 2. Silicate absorption bands at about 1085 (ν), 606 (δ), and 462 (ν_2) cm^{-1} were observed on the spectra of the glasses before soaking. Phosphate absorption bands at about 1043 (ν_3), 963 (ν_1), 603 (ν_4), 566 (ν_4), and 469 (δ) cm^{-1} and carbonate absorption bands at about 1490 (ν_3), 1423 (ν_3), and 874 (ν_2) cm^{-1} were observed on spectra of materials soaked for 7 days. However, the evolution of carbonate bands is somehow slower for **76SA** as it can be observed in the spectra of both glasses after 3 days of soaking, in which carbonate bands are already present in **76S** while they are almost imperceptible for **76SA**. However, the apparition of these bands points to the formation of a carbonate hydroxyapatite, since they are similar to those observed in the synthetic carbonate hydroxyapatite (CHA).[10] The appearance of the phosphate and carbonate absorption bands in the spectra of the materials formed on glass surfaces after soaking in SBF solution not only confirms the formation of an apatite-like layer but also determines that the newly formed material is a carbonate hydroxyapatite, similar to biological apatites in which a coupled substitution of Ca^{2+} and CO_3^{2-} for PO_4^{3-} is observed.[15,16]

(15) Kokubo, T. *An introduction to bioceramics. Advanced series in ceramics, Vol. 1*; Hench, L. L., Wilson, J., Eds.; World Scientific Publishing Co.: Singapore, 1993; pp 75−88.

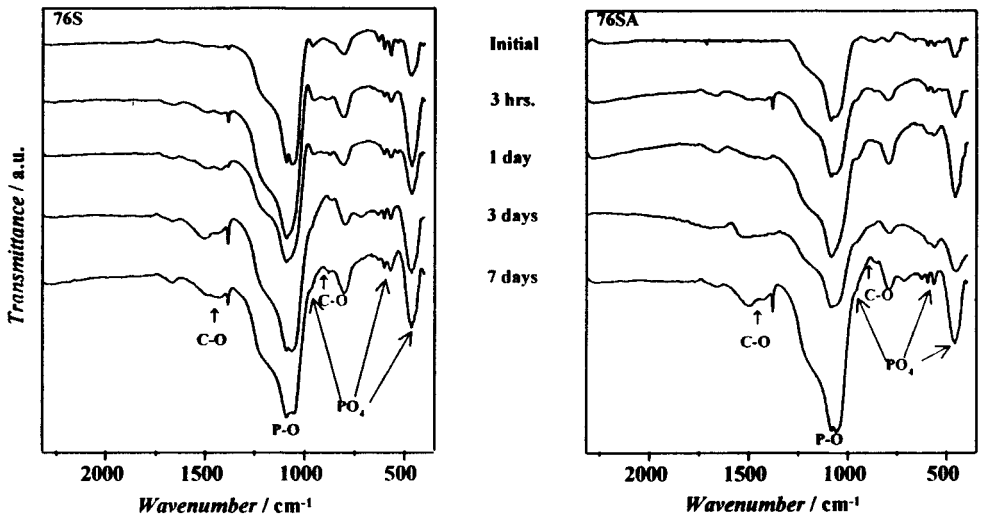

Figure 2. FTIR spectra obtained for **76S** and **76SA** before and after soaking in SBF.

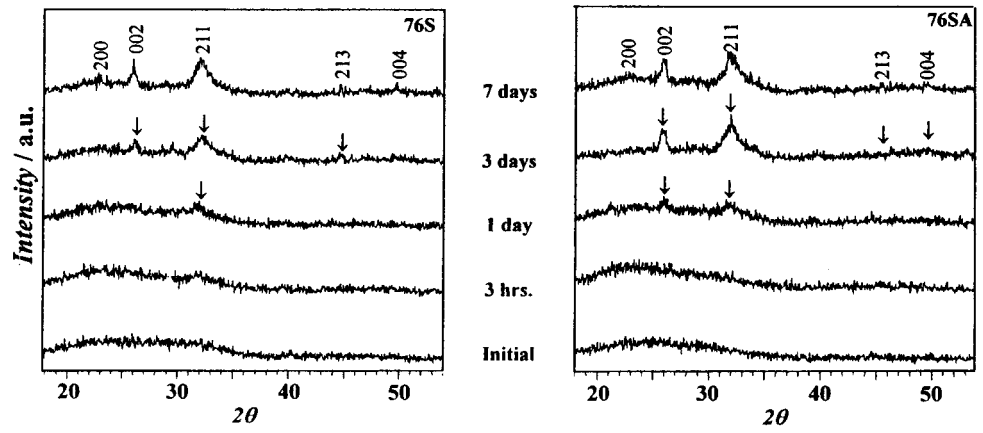

Figure 3. XRD pattern of **76S** and **76SA** before and after soaking in SBF.

Figure 3 shows XRD patterns of glasses **76S** and **76SA** before and after soaking in SBF. In both cases, the glasses show the characteristic wide band at 20−30° (2θ) of amorphous material, and it is after 24 h of soaking when appreciable changes are observed. At that time, **76S** exhibits a slight maximum that could correspond to (211) reflection of an apatite-like phase. With longer soaking times, this reflection becomes sharper and other reflections are detected as well: (200), (211), (213), and (004), all of them suitable to an apatite-like phase. The case of **76SA** is similar although the reflection (002) is already appreciable in the pattern of glass soaked for 24 h. These dates point to the formation of an apatite-like layer on the glass surface if we consider the ASTM-74-0565 as the reference (hydroxyapatite, $P6_3/m$).

SEM micrographs of **76S** and **76SA** before and after different soaking times are shown in Figure 4. The as-obtained materials have different morphologies depending on the precursor employed in the synthesis; the **76SA** surface is more compact and homogeneous. It exhibits a stronger interparticle union, leading to a smaller space between particles than **76S**. When **76S** is immersed in SBF for 3 h, isolated spherical particles are detected on its surface. After 24 h of immersion, these particles grow in size reaching 2−2.5 μm in diameter, and after 3 days of assay, it can be observed that they are constituted by hundreds of crystalline aggregates. This morphology does not further change with soaking time although the size of aggregates increases. Besides, **76SA** soaked in SBF also presents a similar behavior although some differences should be pointed out. After 3 h of immersion, the glass surface is covered by a layer of small spherical particles smaller than 0.3 μm in diameter, some of which reach the size of 0.5 μm after 24 h of soaking. After 3 days, these particles are constituted by hundreds of needlelike crystalline aggregates and they homogeneously cover the entire surface of the glass. This behavior is different from that observed for **76S**, in which the layer also covered the surface but its morphology was irregular. Nevertheless, comparison between micrographs after 3 h of soaking reveals how the growth of the apatite layer on **76SA** is uniform while in case of **76S**, only spherical clusters are observed. These latter grow building the apatite-like layer that covers the glass surface within 24 h.

In addition, the higher degree of homogeneity of the newly formed layer on the **76SA** surface is revealed in micrographs of material soaked for 3 and 7 days, in which the spherical particles can hardly be distinguished and an uniform mantle of needlelike crystalline aggregates is present. However, these particles are

(16) LeGeros, R. Z. *Prog. Cryst. Growth Charact. Mater.* **1981**, *4*, 1.

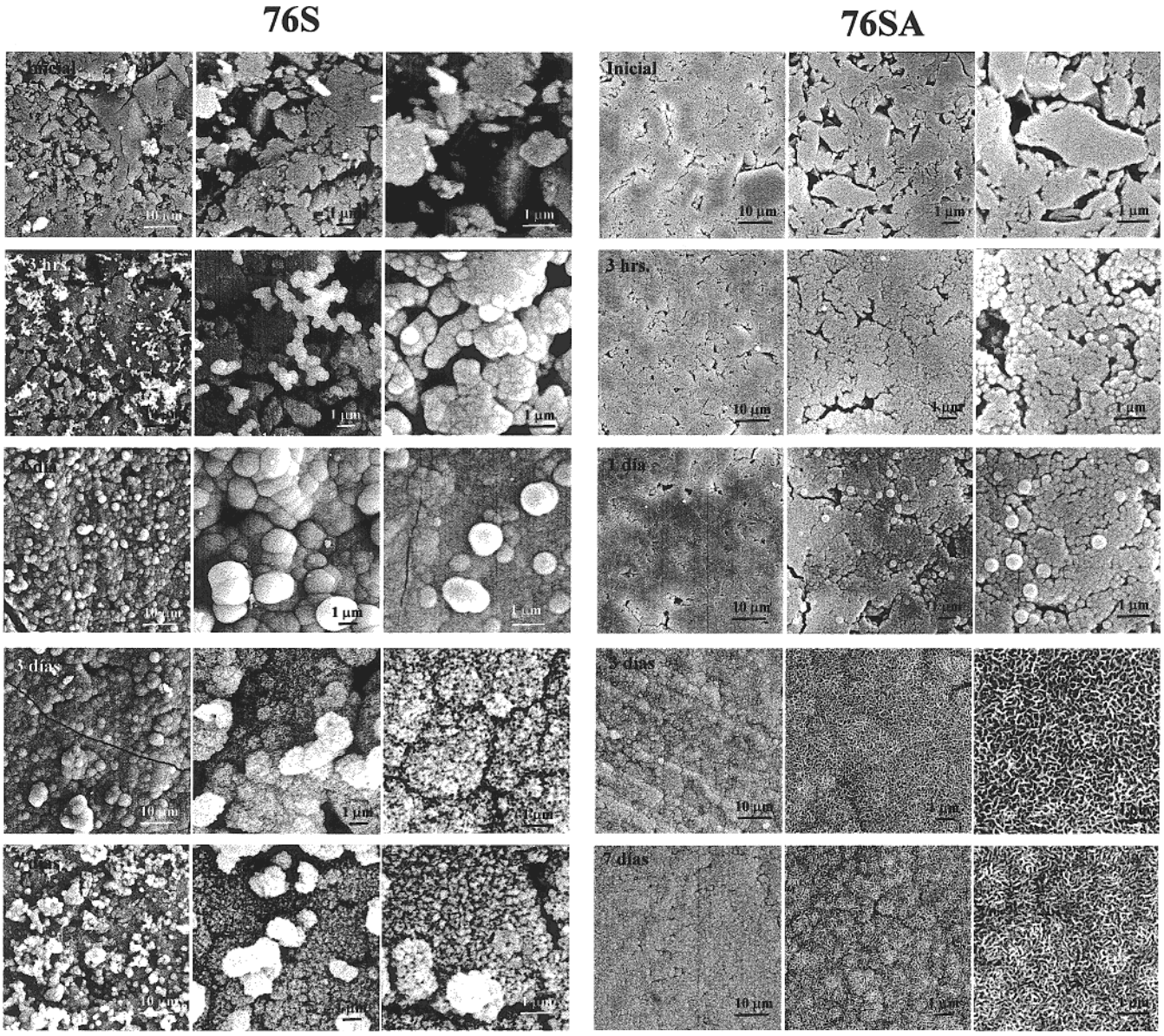

Figure 4. SEM micrographs obtained for **76S** and **76SA** before and after soaking in SBF.

discernible in micrographs of **76S** at the same soaking time.

It is remarkable that the aspect of the **76SA** surface after 7 days of assay is comparable with that shown by other glasses of similar composition after 15 days of soaking in SBF. Generally, these glasses behave like **76S**; that is, the apatite-like formation occurs in two stages: a previous formation of spherical particles followed by the apparition of the needlelike crystalline aggregates, which is after 15 days when these particles begin to be indistinguishable.[17]

The comparison of the results obtained for both glasses points to a disperse nucleation of an apatite phase on **76S** which leads to the growth of spherical clusters that can be detected from the first hours of the assay and are heterogeneously distributed over **76S** surface. The individual growth of these clusters leads to the layer formation. Instead, **76SA** seems to nucleate homogeneously so that the observed layer is formed from a larger number of crystallization nuclei individually distributed (no clusters). This could be the reason why spherical particles displayed in micrograph of **76S** at 24 h of assay are about five times bigger than those present on **76SA** surface (2−2.5 and 0.3−0.5 μm, respectively).

In Figure 5 cross sections of both **76S** and **76SA** after 7 days of assay are shown. The EDS spectra inside the glass and on the layer are also included. As observed, the analysis of the inner part agrees with the nominal composition, i.e., 76% SiO_2, 23% CaO, and 1% P_2O_5 (mol %) in both glasses. However, in the EDS spectra of the layer, a remarkable increase of Ca and P concentration, together with a significant decrease of Si, was observed. The decrease of Si with the increase of Ca and P concentrations indicates the formation of an apatite-like material. In addition, **76S** still displays a small amount of Si on its EDS pattern of the layer, whereas in the case of **76SA**, Si is not perceptible. This fact could be

(17) LeGeros, R. Z.; LeGeros, J. P.; Trautz, O. R.; Klein, E. *Dev. Appl. Spectrosc.* **1970**, *7B*, 13.
(18) Pérez-Pariente, J.; Balas, F.; Salinas, A.; Román, J.; Vallet-Regí, M. *J. Biomed. Mater. Res.* **1999**, *47*, 170.

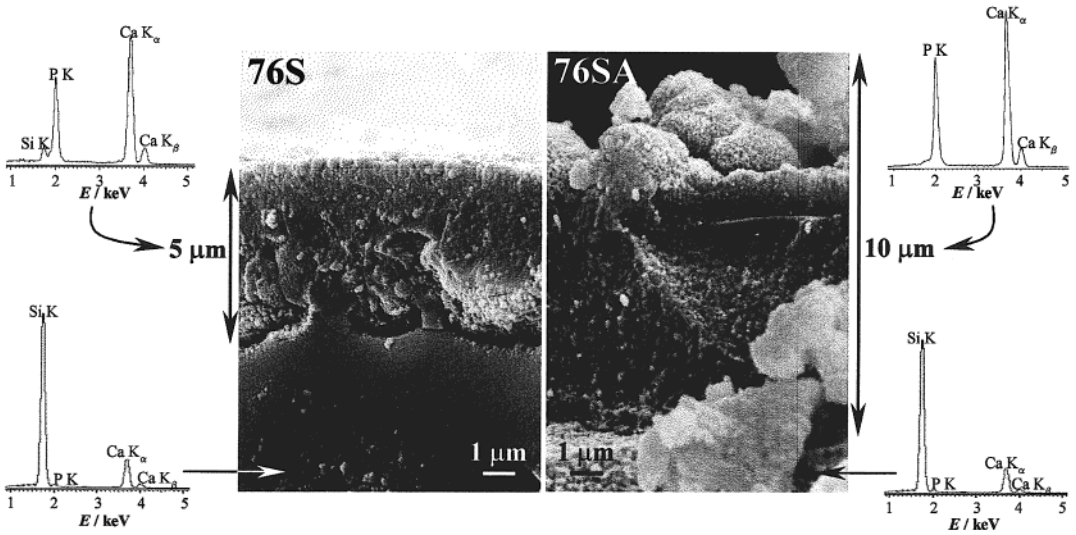

Figure 5. SEM micrographs of the cross section of **76S** and **76SA** soaked in SBF for 7 days and the EDS patterns of the inside of the glasses and of the layer.

related to the different thicknesses of both layers. Analysis of the **76S** layer could partially include the glass underneath it, while for **76SA**, this is less feasible since the newly formed layer is thicker.

On the other hand, the thickness of the **76S** layer is about 5−6 μm whereas for **76SA**, it reaches the value of 8−10 μm. In addition, the micrograph of the **76S** section shows a separation between the glass and the layer formed on it, while this layer seems to be more tightly linked to the glass in **76SA**. This fact agrees with above SEM observations in which **76SA** showed a more homogeneous nucleation that would lead to the larger number of links between the glass and the formed layer. Nonetheless, the heterogeneous nucleation of **76S** causes the union of the layer with the glass to be strong only in nucleation sites, and when the layer expands laterally, until the surface is covered, the newly grown layer is not linked to the glass.

Variations in SBF Composition. Changes in SBF composition that took place during the in vitro assay for both **76S** and **76SA** are shown in Figure 6. The rapid release of Ca^{2+} from **76S** in the first hours of assay and the subsequent decrease of Ca^{2+} after 1 day of soaking in the solution can be observed, whereas this release is observed to be smoother and continuous for **76SA**. These variations in Ca^{2+} are accompanied in both cases by a decrease in P content of the solution and increase in pH, as it can be observed in parts b and c of Figure 6. These observations point to an apatite-like layer formation that is in agreement with the Kokubo mechanism,[6] which can be explained in terms of a chemical reaction taking place between the glass and the solution. When the glass gets in contact with the SBF, a partial dissolution occurs, producing an ionic interchange of Ca^{2+} of the glass with H_3O^+ of the media. This leads to an increase of both ionic concentration and pH of the media together with the formation of silanol groups on the glass surface. This latter fact enhances the creation of crystallization nuclei for the hydroxyapatite, which can be formed from the high concentration of Ca^{2+} and PO_4^{3-} present in the media. In summary, a chemical reaction takes place between the glass and the SBF, with formation of apatite being the reaction product.

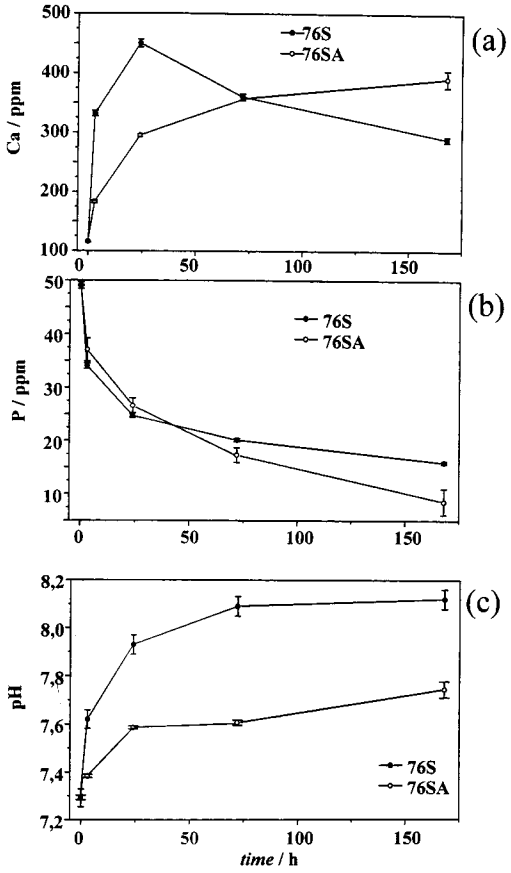

Figure 6. Changes produced in SBF as a function of soaking time for **76S** and **76SA**: (a) changes in Ca^{2+}, (b) changes in P, and (c) changes in pH.

The differences in rate release of Ca^{2+} into the media from both **76S** and **76SA** is related to the different behaviors of layer formation on glass surface. The rapid supersaturation of the media in case of **76S** leads to the constitution of clusters observed in Figure 4, while when Ca^{2+} is continuously released from **76SA**, the formation of the layer is more homogeneous.

Study of Porosity. To study the textural properties of the glass synthesized from both calcium nitrate and alkoxide, a study of porosity was carried out by Hg

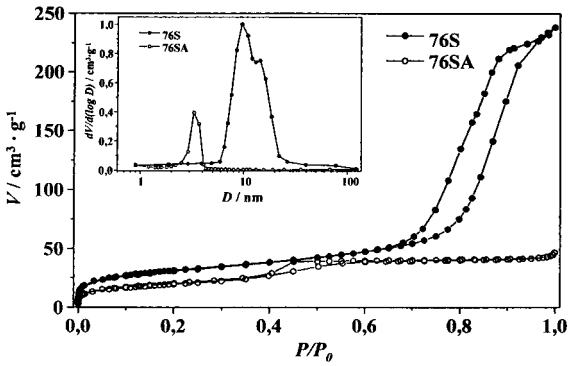

Figure 7. Nitrogen adsorption isotherms of **76S** and **76SA** and pore distribution.

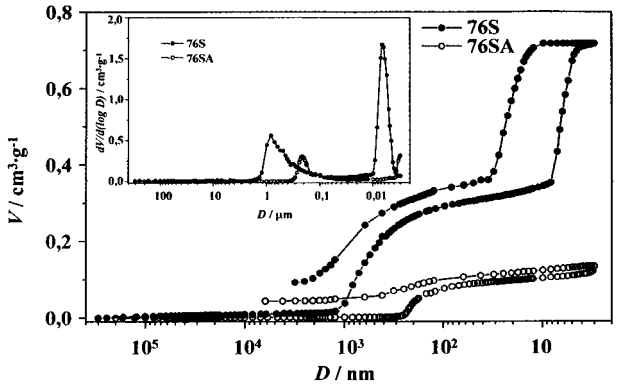

Figure 8. Hg intrusion curve of **76S** and **76SA** and pore distribution.

intrusion and N_2 adsorption. Also, the changes in porosity during the in vitro assay were followed to establish the development of the layer formation.

In Figure 7, nitrogen adsorption isotherms of **76S** and **76SA**, before soaking, together with their pore distributions are shown. It can be observed that **76S** displays a wide maximum band centered at 8.5 nm with a shoulder at about 12 nm, while **76SA** exhibits a narrower distribution of mesopores that are 3.3 nm in diameter. This seems understandable taking into account the micrographs obtained for both materials before soaking in SBF, in which bigger pores were observed for **76S** than for **76SA**, and the latter showed a higher degree of homogeneity.

Figure 8 shows the results obtained by Hg intrusion for **76S** and **76SA,** before soaking in SBF, and the pore distributions in the corresponding range of pore diameter. While **76S** displays two different sizes of pores (macropores, 2000−200 nm; mesopores, 30−3 nm) with their maxima at 820 and 6.4 nm, respectively, **76SA** exhibits a single maximum at 180 nm in the region that can be suitably measured by this method. However, a second maximum seems to appear at about 3 nm, according to the results obtained by nitrogen adsorption. Hence, there is a textural difference between the two glasses not only in homogeneity, as discussed above, but also in pore size distribution. Also, the pore volume is different, being quite higher for **76S** (0.72 cm^3g^{-1}) than for **76SA** (0.13 cm^3g^{-1}).

These different textures of **76S** and **76SA** must be due to the synthesis method since that is the only difference between them. The final step of the sol−gel method for **76S** implies heating at 700 °C to remove the nitrates present in the gel. During the $Ca(NO_3)_2$ decomposition, new porosity is generated in addition to the already existent porosity in glass owing to the structure itself.

These differences in porosity of the starting material could be responsible for the different in vitro behavior observed for the two glasses. In fact, it is possible to explain the results obtained in terms of porosity.

The diagram of calcium release presented in Figure 6 shows a higher rate of release for **76S** with respect to **76SA**. This could be due to the macropores present in the **76S** structure, which increase surface contact with the fluid and therefore favor the glass dissolution. Hence, during the first hours, this release is fast and when the Ca^{2+} concentration reaches its maximum value of almost 450 ppm, this concentration starts to decrease at the expense of the formation of the new apatite layer. Nonetheless, since **76SA** has smaller pores, its release of Ca^{2+} to the media is slower but continuous, in agreement with its homogeneity.

The evolution of porosity during the in vitro assay is shown in Figure 9, in which the pore distribution of glasses **76S** and **76SA** after different times of soaking in SBF is displayed. Since **76SA** exhibits only one maximum, which belongs to the macropore region, comparison of pore evolution is made in that section in particular. Figure 10 shows evolution of both diameter of pores and porosity percentage. As it can be observed, the diameter of **76S** macropores increases in the first day, which can be due to the loss of Ca^{2+} to the media, and subsequently decreases. This fact can be attributed to layer formation and consequent pore filling. In case

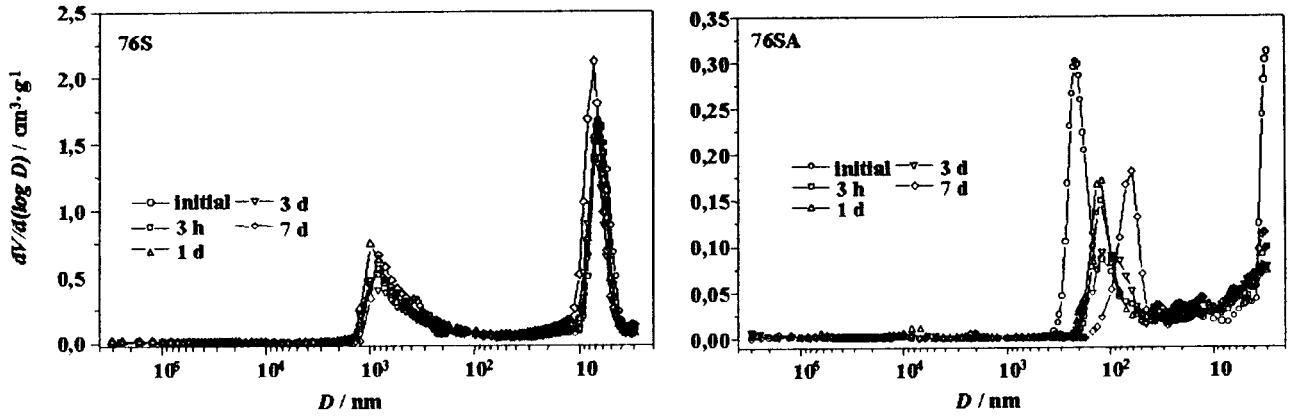

Figure 9. Evolution of pore distribution as a function of soaking time in SBF for **76S** and **76SA**.

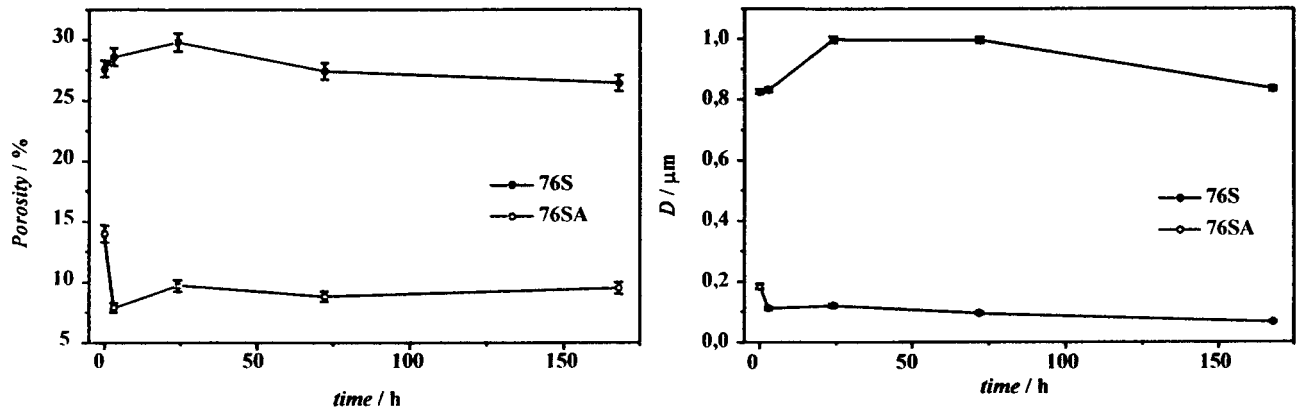

Figure 10. Evolution of porosity and diameters of pores of **76S** and **76SA** during in vitro assay.

of **76SA**, pore size starts decreasing from the beginning of the assay according to the homogeneous covering of the surface. As expected, porosity evolution presents a similar tendency as pore diameter for both glasses.

Conclusions

A new bioactive glass was synthesized by sol−gel method, following two different procedures: inorganic and organometallic routes. In both cases, the glass obtained exhibited good bioactivity.

The alkoxide route allowed the performance of the glass synthesis at lower temperatures than the traditional method.

After few hours of assay, spherical particles found on glass surfaces are smaller for **76SA** but they are homogeneously distributed all over the surface. Besides, after longer times of soaking in SBF, the covering of the surface seems denser for the glass synthesized via metal alkoxides, which is revealed by the higher thickness of the apatite-like layer. In addition, the homogeneous nucleation of this apatite on the surface leads to a better bond between the glass and the newly formed layer.

In summary, both methods employed in the synthesis of the glass lead to a good bioactivity although the glass obtained via metal alkoxide exhibits better structural and textural properties.

Acknowledgment. The authors acknowledge Dr. Pérez-Pariente for the discussion of the porosity results. The authors are grateful for financial support provided by MAT99-0466.

CM0110876